Mon. Not. R. Astron. Soc. **265**, 471–485 (1993)

Observations of type II plateau supernovae: SNe 1988A, 1988H and 1989C ★

M. Turatto,[1] E. Cappellaro,[1] S. Benetti[2] and I.J. Danziger[3]
[1]*Osservatorio Astronomico di Padova, vicolo dell'Osservatorio 5, I-35122 Padova, Italy*
[2]*Dipartimento di Astronomia, Università di Padova, vicolo dell'Osservatorio 5, I-35122 Padova, Italy*
[3]*European Southern Observatory, Karl-Schwarzschild-Strasse 2, D-8046 Garching bei München, Germany*

Accepted 1993 June 10. Received 1993 May 12; in original form 1993 March 1

ABSTRACT

We present new photometric and spectroscopic observations of three type II supernovae with plateau light curves: SNe 1988A, 1988H and 1989C.

From the new photometry of SN 1988A, we do not confirm the previous claim of a departure of the late-time light curve from ^{56}Co radioactive decay and thus have no indication of the emergence of an additional source of energy. The early spectral evolution of SN 1988A seems rather normal, but for the appearance of a blue emission-like feature on the Hα profile resembling a similar feature detected in SN 1987A. As in that supernova, this may be a manifestation of the appearance of radioactive ^{56}Co above the photosphere. In the late-time spectrum (~ 450 d) several emission lines are identified. Apart from the lines of H, [O I], Ca II, Ca II], Na I and Mg I], many of the other lines are probably due to Fe II and [Fe II].

In the late spectrum of the plateau SNII 1988H, we find that the positions of the peaks of the broad lines are blueshifted with respect to the rest-frame positions, and that the line profiles are asymmetric with a deficiency of radiation in the red wings. We suggest that this is evidence for dust formation within the supernova envelope. The fact that in SN 1988H this phenomenon occurs relatively early (about 300 d earlier than in SN 1987A) may be related to the greater expansion velocity and spectral evolution of this SN.

SN 1989C has been proposed as a member of the class of SNII with narrow lines (SNIIn). We find that published magnitudes are heavily affected by the light of the nearby galaxy nucleus. The revised photometry and the new photometry place this SN among the plateau SNII with faster photometric evolution. Analysis of the spectroscopic observations shows a low expansion velocity, as determined from the Hα absorption, similar to the expansion velocity derived from Fe II lines. This may indicate an unusually small Hα optical depth for this SN. Also, we note that the narrow lines, present on the spectra, are more likely to be due to an underlying H II region.

Key words: supernovae: general – supernovae: individual: 1988A – supernovae: individual: 1988H – supernovae: individual: 1989C – supernova remnants.

1 INTRODUCTION

The most frequent supernovae (SNe) in spiral galaxies are of type II (Cappellaro et al. 1993). However, because of the lower absolute luminosity and the association with regions of high extinction, the number of type II supernovae (SNII) discovered is smaller than that of type I supernovae (SNI).

Only a few SNII have merited extensive observations, probably because the low brightness and the contamination by the SN surroundings make the observations, especially at late epochs, rather difficult. In the last decade the situation has considerably improved, thanks to the use of linear detectors, modern reduction techniques and the allocation of large telescopes to SN programmes.

Recent observations confirm that objects with quite different characteristics are included in the class of SNII. One of the most outstanding cases is SN 1988Z (Turatto et al. 1993), which should be considered the prototype of a separate subclass of SNII, named SNIIn (Schlegel 1990; Stathakis & Sadler 1991). However, even within the most *normal* SNII, significant differences exist in both the photometric and the

★ Based on observations collected at Asiago (Italy) and ESO-La Silla (Chile).

Table 1. Main data on SNe 1988A, 1988H and 1989C.

SN	1988A	1988H	1989C
host galaxy	NGC 4579	NGC 5878	UGC 5249
R.A. (1950)	$12^h35^m12^s.6$	$15^h10^m59^s.4$	$9^h45^m09^s.8$
Dec. (1950)	12°05′40″	−14°05′05″	2°51′35″
distance mod.*	31.13	32.50	32.21
A_B*	0.10	0.47	0.12
	heliocentric recession velocity		
host galaxy*	1805	2111	1882
SN location	1550	2170	1950
offset from galaxy nucleus [arcsec]	0.5W 46.1S	22W 55N	1.5E 0.7S
J.D.(max)(24...)	47180	47224:	47560:
m_V(max)	13.5	≤ 16.2	≤ 15.0
M_V(max)	−17.7	≤ −16.7	≤ −17.3
light curve	plateau	plateau	plateau

* From the Nearby Galaxies Catalog (Tully 1988).

spectroscopic evolutions.

The present paper deals with the results of observations of three SNII (1988A, 1988H and 1989C, see Table 1) up to the limits of detection by the largest European telescopes. In the following sections it is shown that a careful analysis of the photometry casts some doubts on previous claims concerning the SNe studied in this paper. Also, we show that important results have been obtained from good signal-to-noise ratio low-dispersion spectrophotometry of SNII older than 1 yr, concerning the input energy source, dust formation and nucleosynthesis.

2 OBSERVATIONS AND REDUCTIONS

The early-epoch observations discussed in this paper were obtained at the Asiago Observatory, while the latest observations were obtained at ESO-La Silla. Throughout this paper, the ages of the SNe are referred to the date of the *B* maximum light.

2.1 Photometry

The photometry was performed with the CCD cameras at Asiago and the 1.5-m Danish telescope at La Silla, or by means of the ESO Faint Object Spectrographs and Cameras (EFOSC1 and EFOSC2) at the 3.6-m and at the New Technology Telescope (NTT) (Table 2). In all cases, a number of Landolt's (1983) stars were used for calibration.

For SNe 1988H and 1989C we also obtained a few plates with the Asiago 67/92-cm Schmidt telescope. For the *B* band we used 103aO Kodak emulsion and a GG13 filter, and for *V* band we used 103aD and GG14. The SN magnitudes were estimated by visual comparison against CCD-calibrated field stars.

The frames were analysed with the ROMAFOT package in the MIDAS environment. This code, originally designed for

Table 2. Photometric observations.

Date	J.D. 2400000	B	V	R	equipment
		SN 1988A*			
8/3/89	47593.5	20.75	20.00	19.60	Dan154
26/2/90	47948.5	>22.6	>23.0	>22.0	Dan154
18/3/90	47968.5	>22.6	>22.9	>22.5	NTT
		SN 1988H			
12/3/88	47232.5	17.35			S67
16/3/88	47236.5		16.2		AS182
23/3/88	47243.8		16.15		Dan154
16/4/88	47267.5	17.75			S67
18/4/88	47269.5	17.65	16.40		AS182
8/4/89	47624.9	22.40	21.55	21.10	EFOSC1
28/4/89	47644.6		21.90	21.45	Dan154
26/2/90	47948.6		>22.2	>21.4	Dan154
		SN 1989C			
7/2/89	47564.5	15.15	15.40		S67
9/2/89	47566.4	15.20			S67
10/2/89	47567.5		15.40		S67
7/4/89	47623.6	16.65	16.05	15.70	EFOSC1
28/4/89	47644.5	18.00	17.00	16.45	Dan154
27/10/89	47826.5		>19.8	>20.2	AS182
25/2/90	47947.5		>20.5	>20.4	Dan154
18/3/90	47968.5			>20.0	NTT

* For earlier photometry see Benetti et al. (1991).
AS182 = Asiago 1.8–m + CCD; Dan154 = ESO/Danish 1.5–m + CCD; EFOSC1 = ESO 3.6–m + EFOSC1; S67 = Asiago 67/92–cm Schmidt; NTT = ESO NTT + EFOSC2.

stellar photometry in crowded fields, is very useful for our purpose, mainly because of the interactive options. The reduction pipeline starts from the determination of an analytical approximation of the point spread function (PSF) from field stars. Then the two-dimensional subarray containing the target object is fitted by the sum of elementary PSFs, each representing an individual star. The sky contribution is taken into account with an analytical plane, possibly tilted, which is fitted simultaneously with the stars. It is also possible to mask any feature that does not have to be fitted.

We illustrate the application of this method to the case of SN 1989C, which appeared projected very close to the galactic nucleus and is a typical case for which aperture photometry is not reliable. In Fig. 1 are shown, for a *V* frame of SN 1989C, (a) the original observation, (b) the fitted image and (c) the residual. From the residual map, one can judge how well the fit works. In fact, a small residual is left at the SN position due to a slight (~ 10 per cent) elongation of the stellar images in the north–south direction, not accounted for by the symmetric approximation of the PSF. If we neglect this second-order effect, it appears that the contribution from the host galaxy is very well subtracted. We note that, compared with *cruder* aperture photometry, the measured magnitude of this SN is 0.5–0.9 mag fainter, depending on the size of the aperture. We

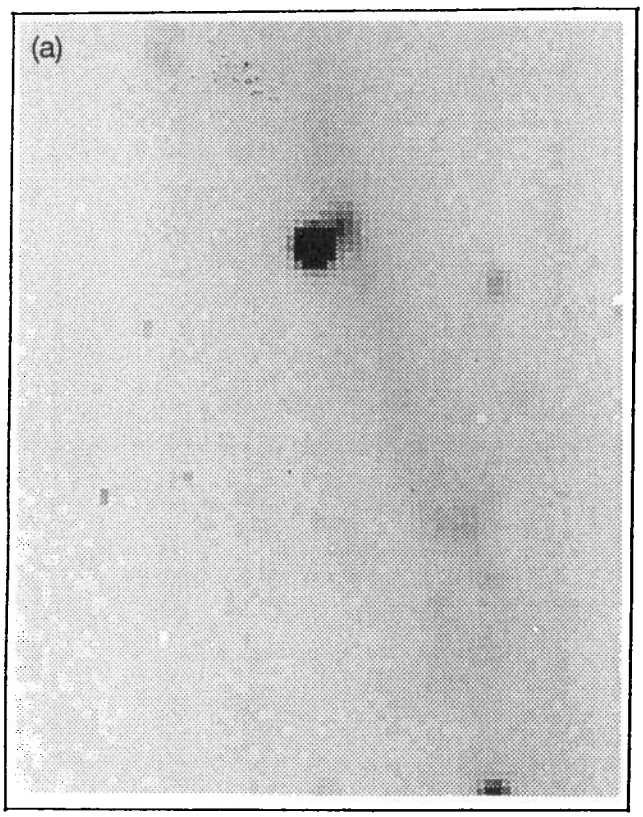

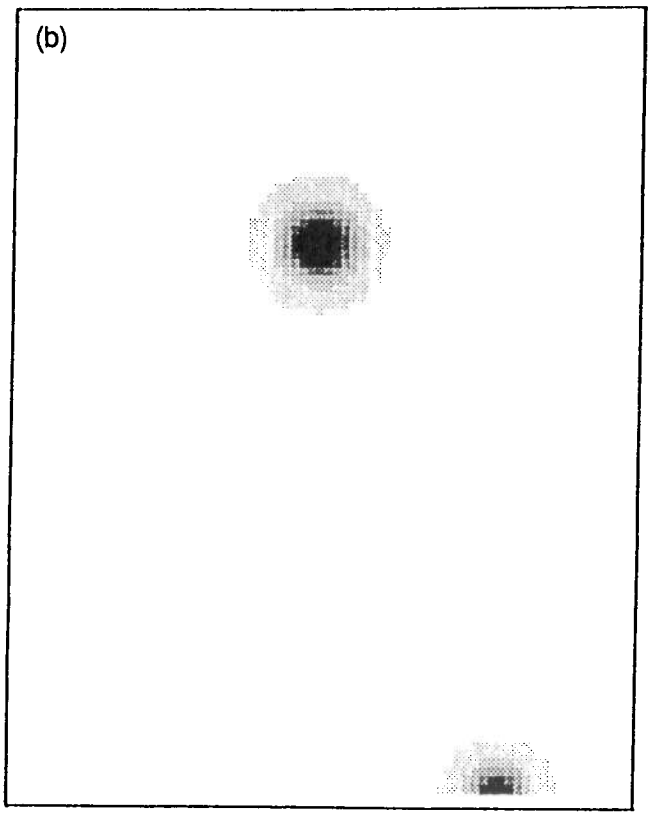

Figure 1. Example of photometric measurements with ROMAFOT: (a) *V* frame of SN 1989C taken on 1989 April 28 (seeing FWHM= 1.4 arcsec); (b) fitted stellar objects; (c) residual map after subtraction of the fitted stars from the original frame. North is at the top, east to the left. The SN is the bright object south-east of the galaxy nucleus.

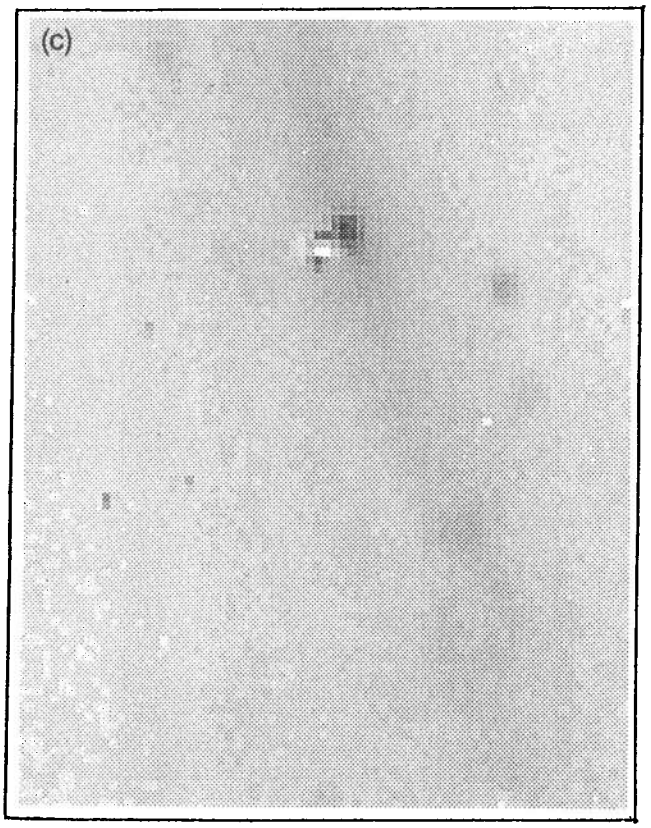

Figure 1 – *continued*

believe that our use of this method can explain the discrepancy between our estimates and those of other authors (cf. Section 4.3).

When we did not detect the SN, an *accurate* upper limit has been given. This was determined by placing, at the precise location of the SN, artificial stars of successively decreasing brightness, and taking as an upper limit the magnitude of the faintest star that we deemed recoverable.

The errors of the photometry depend on the object brightness and on the local galaxy background. For the SNe measured here, these errors range from 0.05 to 0.3 mag in the most unfavourable cases.

2.2 Spectroscopy

The journal of the spectroscopic observations is reported in Table 3. The CCD spectra taken at Asiago with the Boller & Chivens spectrograph at the 1.8-m telescope (resolution of about 6 Å) are combinations of a few exposures at different grating inclinations. Also, the late-time EFOSC spectra result from the merging of B300 and R300 grism spectra (resolution $\sim$ 20 Å). Sometimes, spectra taken on consecutive nights were added in order to improve the signal-to-noise ratio. In all cases, the cumulative exposure time is indicated.

The wavelength calibration was performed with adjacent exposures of comparison lamps, and flux calibration was carried out via observations of spectrophotometric standard stars. The flux calibration of the spectra was checked and found to be in fair agreement with broad-band photometry.

Table 3. Journal of the spectroscopic observations.

Date	epoch (days)	range Å	equipment
	SN 1988A		
8/3/1988	49	3830–7400	AS182
25-28/3/1988	67	4090–6900	AS182
20-21/4/1988	92	4180–7570	AS182
7/4/1989	444	4000–9200	EF1
	SN 1988H		
25/3/1988	42	4700–6900	AS182
20-21/4/1988	68	4700–6900	AS182
5-6/4/1989	418	4000–9200	EF1
	SN 1989C		
11/2/1989	8	4000–7200	AS122
29-30/3/1989	55	4700–6800	AS182
7/4/1989	64	3900–6800	EF1

AS122 = Asiago 1.2–m + AVI; AS182 = Asiago 1.8–m + B&C; EF1 = ESO 3.6–m + EFOSC1 (B300+R300).

The early spectrum of SN 1989C was obtained with the prismatic spectrograph at the 1.2-m telescope at Asiago. An RCA image tube and Kodak 103a-O plate were used as detector (resolution ~ 4 Å at Hβ). The image was digitized with the PDS spectrodensitometer and transformed to relative intensity and finally placed on an absolute scale using the photometry.

3 SOME GENERAL ASPECTS OF SNe 1988A, 1988H AND 1989C

SN 1988A has been observed extensively and its photometric evolution has been studied in several papers (e.g. Benetti et al. 1991). In the first 400 d after the discovery it showed the characteristic behaviour of SNII with *plateaux*, resembling both in *B* and in *V* the light curve of the typical SN 1969L. In particular, for these two SNe the durations and the slopes of the plateaux are similar, indicating similar structures of the envelope. On the other hand, SN 1988A began with an initial luminosity spike possibly similar to that which occurred in SN 1987A.

SN 1988H appeared in the outer regions of the nearly edge-on Sb galaxy NGC 5878 (incidentally, note that the position angle reported by the major catalogues, PA= 90°, is wrong because the major axis of NGC 5878 is oriented almost north–south). This is unexpected for SNII, considered the progeny of massive stars, even if not unprecedented (e.g. SN 1986E, Cappellaro et al. 1990). However, SN 1988H appeared in an H II region, which is expected to be rich in young stars.

SN 1989C was discovered at $m_{pg} = 14.5$ on 1989 February 3 (Wild 1989) near the centre of the edge-on galaxy MGC+01-25-025 (UGC 5249) (Fig. 1). A study of its early photometry has been published by Kimeridze & Tsvetkov (1991), and a spectrum near maximum light has been presented by Schlegel (1990), who included SN 1989C among the type IIn SNe. According to Schlegel, this class of SNe is characterized by the absence of the P Cygni profile in the Balmer lines and by emission lines with both a broad and a narrow component, the latter probably due to contamination by a surrounding H II region.

Probably because of its location very close to the nucleus of the host galaxy, the offset of SN 1989C was not given. On our CCD frames we measured an offset of 0.7 arcsec south and 1.5 arcsec east.

For each SN, the heliocentric recession velocities at the location of the SN have been measured using the narrow lines of adjacent emission regions. Listed in Table 1, they are consistent with the redshifts of the parent galaxies as reported in the Tully (1988) catalogue. In rows 9–11 of Table 1 are presented also the dates and the magnitudes of the SNe at maximum, as deduced in Section 4.

4 LIGHT CURVES

4.1 The late-time luminosity decay of SN 1988A

It has been shown that the luminosity decline rates of SN 1988A up to 400 d after maximum were in good agreement with the average value for SNII (Turatto et al. 1990). Ruiz-Lapuente et al. (1991) later claimed the detection of an excess of radiation, with respect to the ^{56}Co decay input energy, 700 and 900 d after the explosion. If real, the departure from the ^{56}Co decay implies an additional source of energy.

While monitoring another bright SN in the same host galaxy, SN 1989M, we have been able to determine the photometric behaviour of SN 1988A until 800 d. The results are reported in Table 2, and the observations and the lower limits are reported in Fig. 2 along with the data from Ruiz-Lapuente et al. (1990, 1991). Starting near day 400, our *V* and *R* observations are significantly fainter. These differences are particularly pronounced for the *R* magnitudes. Near 400 d our estimates are already about 1 mag fainter than those of Ruiz-Lapuente et al. (1990), and at 800 d this difference could be larger than 1.6 mag.

Even if strong fluctuations in the late-time light curve cannot be excluded a priori, they have never previously been reported in the light curves of SNe. Therefore we are inclined to ascribe the differences to the data reduction procedure. In fact, in the 1990 frames of SN 1988A we did not find any source with a PSF similar to that of the field stars at the position of the SN. Fig. 3 compares the enlargements of the region of SN 1988A in the *R* frames of 1989 April ($R = 19.7$; Benetti et al. 1991) and 1990 March ($R > 22.5$). Because of the location of the SN on the tip of a bright protuberance, blind aperture photometry, even within small areas and with local background subtraction, might provide unreliable values of the magnitude, as we stressed in Section 2.1.

In conclusion, our photometry does not confirm the departure from the ^{56}Co luminosity decay slope in the late-time light curve of SN 1988A. This in itself does not necessarily prove that the only energy input comes from ^{56}Co, although it might be suggestive. Bolometric light curves are indispensable for arriving at such conclusions.

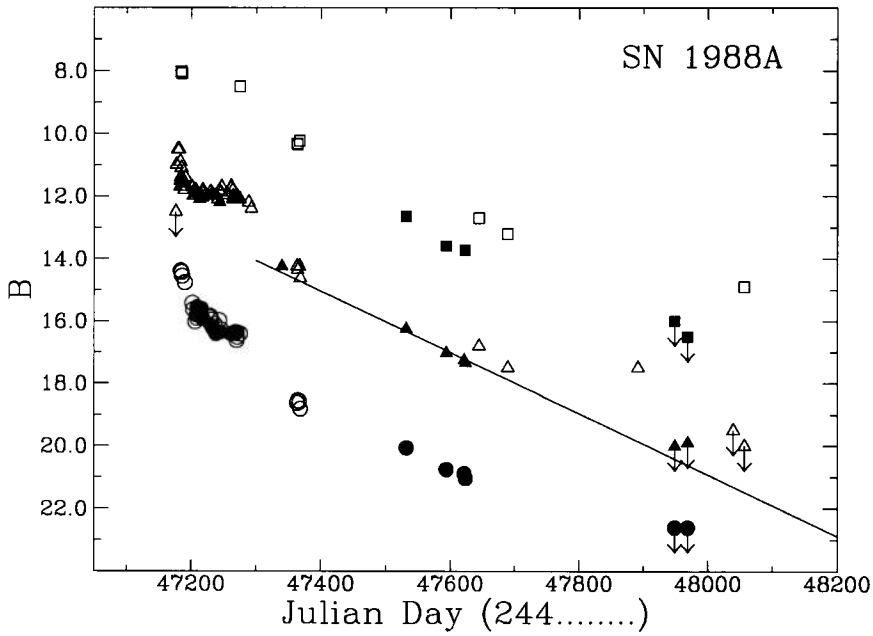

Figure 2. Light curves of SN 1988A in NGC 4579. The vertical scale refers to *B* magnitudes (circles), while *V* data (triangles) have been upward–shifted by 3 mag and *R* data (squares) by 6 mag. Filled symbols are measurements from Table 2 or from Benetti et al. (1991); open symbols are data from literature. The slope of ^{56}Co decay is also drawn.

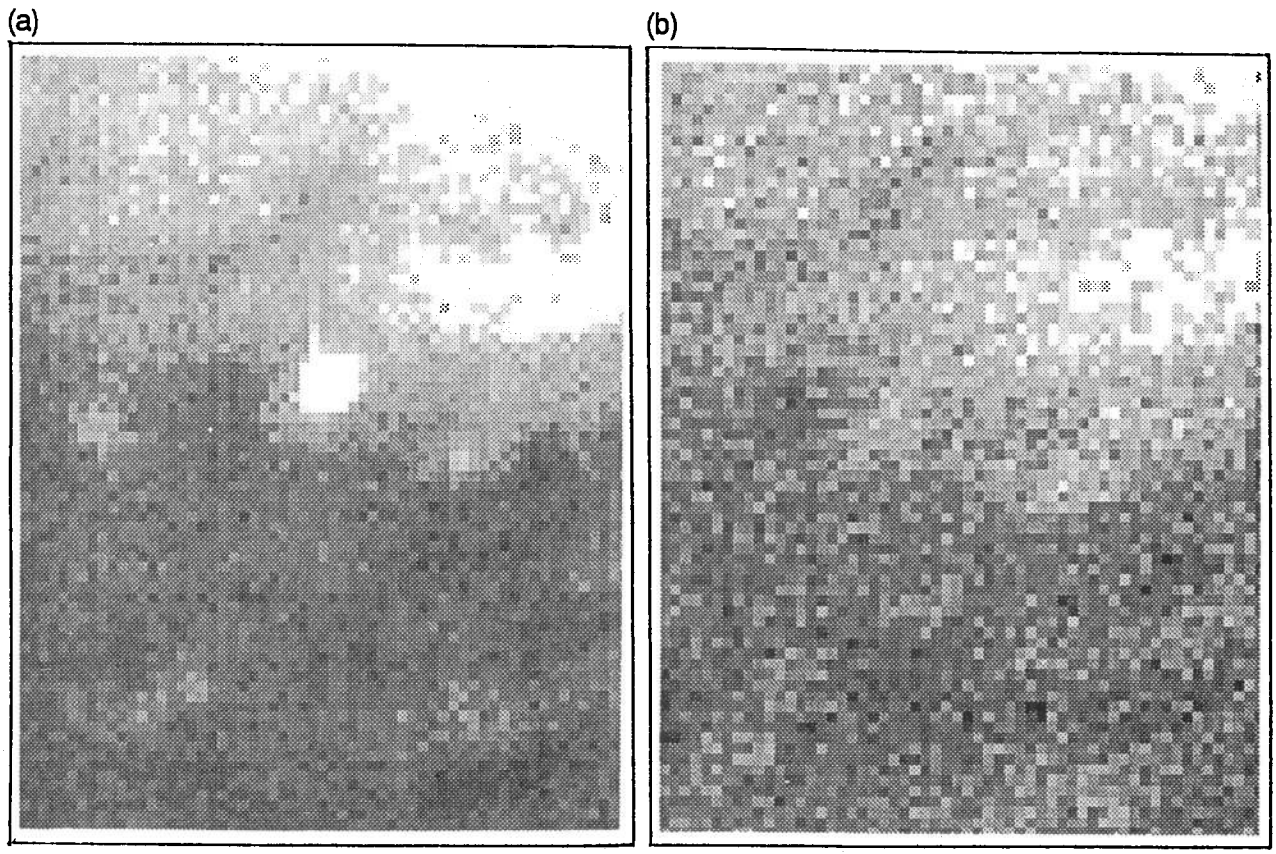

Figure 3. Enlargement of the region around SN 1988A in the *R* band: (a) in 1989 April (when the SN, the bright object in the middle, was at $R = 19.7$); and (b) in 1990 March (the SN was not visible down to a limiting magnitude of $R = 22.5$). For comparison (c) shows how a star at $R = 20.9$ would appear at the position of the SN. North is at the top, east is to the left.

(c)

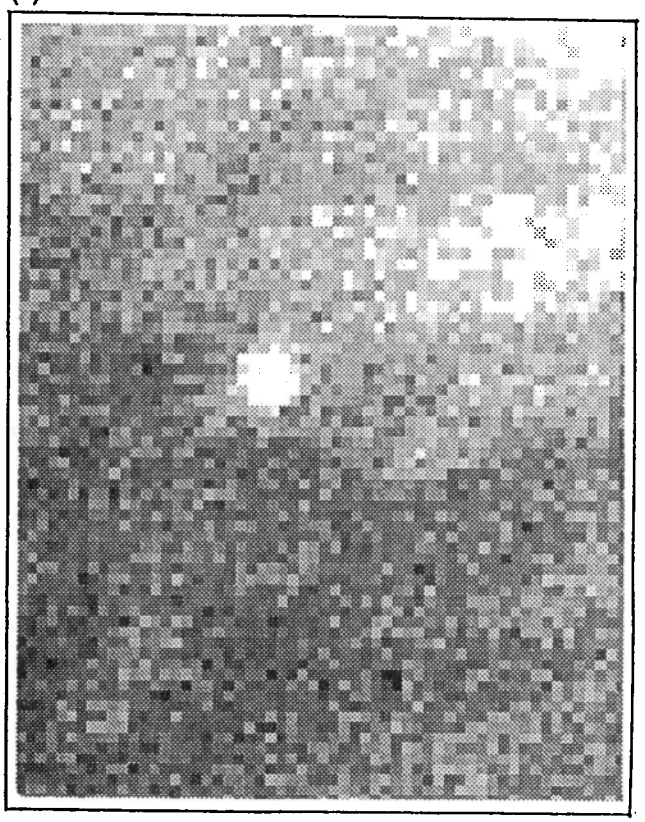

Figure 3 – *continued*

4.2 SN 1988H

The photometry of this SN is scanty. Apart from the early discovery data (Perlmutter et al. 1988), the only additional available photometry is reported in Table 2. These points do not allow one to draw a light curve, but may be useful for the comparison with other SNe. Adopting as reference epoch the day of the early detection by the Berkeley group, i.e. February 12, the comparison of V photometry with the light curve of SN 1988A (a classical example of a plateau SNII) shows a satisfactory correspondence until day 400 (Fig. 4). A similar comparison with the light curve of the *linear* SN 1979C shows that the fading rate in proximity to the maximum is definitely slower for SN 1988H. Therefore it seems reasonable to consider the light curves of SN 1988H to be of the *plateau* type.

Also, SNe 1988H and 1988A show similar $B-V$ colours at the same epochs, suggesting that they suffered a similar small extinction.

In analogy to SN 1988A, we have also determined some limit to the luminosity of SN 1988H at very late epochs. Because of the location of the SN on an H II region, these limits are not particularly deep, but they are consistent with a normal luminosity decline of this SN.

We have also determined the lower limit for the absolute luminosity at maximum of SN 1988H, $M_V \leq -16.7$, which is consistent with the average value for SNII reported by Miller & Branch (1990).

4.3 SN 1989C

In Fig. 5 we show the light curve of SN 1989C which includes, in addition to our measurements from Table 2, the data from the literature. It appears that there is a significant disagreement between our data and the original determinations by Kimeridze & Tsvetkov (1991) (small symbols).

As stressed in Section 2.1, the location of SN 1989C makes the magnitude measurements rather difficult. Especially when the SN brightness declines, the contribution from the host galaxy nucleus needs to be carefully subtracted. This is almost impossible for observations obtained with telescopes with a small scale but, as shown in Fig. 1, can be done fairly well on properly scaled CCD images. We believe that this explains the inconsistencies between our observations and those of Kimeridze & Tsvetkov (1991) (small open symbols in Fig. 5).

In Fig. 5 we have plotted the corrected Kimeridze & Tsvetkov (1991) B magnitudes (large open circles), subtracting the contribution of the host galaxy nucleus as measured on our CCD frames. As expected, near maximum light the correction is very small, but later it becomes important, making the Kimeridze & Tsvetkov observations consistent with our own data.

It is apparent that the luminosity of SN 1989C declined faster than that of SN 1988A. However, it is known that there is a spread in the decline rates even for SNe of the same class. Based on a compilation of type II light curves, Patat et al. (1993) show that the *average* B decline in the first 100 d, β_{100}, is for plateau SNII in the range 1–3.5 mag $(100\,\mathrm{d})^{-1}$, and for linear SNII in the range 4–6 mag $(100\,\mathrm{d})^{-1}$ (neglecting the extreme linear SN 1941A for which $\beta_{100} = 9$ mag $(100\,\mathrm{d})^{-1}$). For SN 1989C we derived $\beta_B = 3.15$ mag $(100\,\mathrm{d})^{-1}$. Therefore it can be considered a fast plateau type, similar to SN 1962M or 1965N.

The maximum absolute magnitude was computed by analogy to the two previous SNe, resulting in $M_V \leq -17.3$.

Late-time observations of SN 1989C after 250 d failed to detect the object. Because of the location within the galaxy, these observations set relatively bright upper limits to the SN luminosity. These limits are consistent with a normally ^{56}Co-powered late–time light curve. Had SN 1989C shared the same properties as other well-studied SNIIn, SNe 1988Z and 1987F, its luminosity decline would have been very slow and the SN easily detectable up to a very late epoch.

When we compare luminosities at similar late phases (> 250 d) assuming that the V luminosity scales with the mass of ^{56}Co, we estimate that SNe 1988A, 1988H and 1989C have produced the same original masses of ^{56}Ni as has SN 1987A.

5 THE EARLY SPECTRA OF THE THREE SNe

5.1 SN 1988A

Only sparse spectroscopic observations have been published to date. The early information comes from the IAU Circulars, which report the observation of a nearly featureless spectrum at maximum with weak P Cygni profiles of Hα and Hβ.

A spectrum is available for epoch 23 d (Pearce et al. 1990; Ruiz-Lapuente et al. 1990). The Balmer lines have well-defined P Cygni profiles superimposed on a strong continuum, as well as Na I and Ca II lines. The resemblance to spectra of SN 1987A is clear (cf. Danziger et al. 1987).

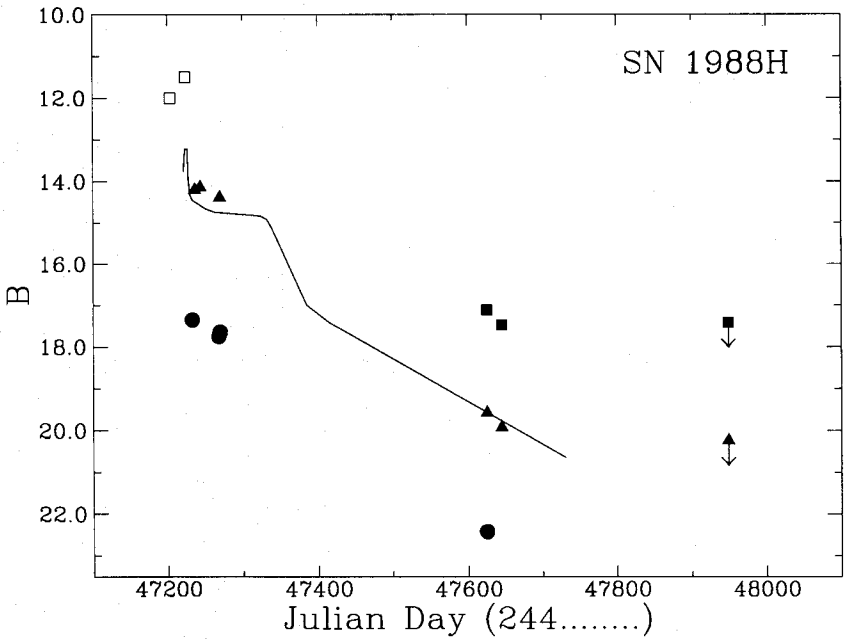

Figure 4. Light curves of SN 1988H in NGC 5878. The vertical scale refers to *B* magnitudes (circles), while *V* data (triangles) have been upward-shifted by 2 mag and *R* data (squares) have been shifted by 4 mag. Open symbols are data from literature. Also shown is a schematic representation of the *V* light curve of SN 1988A, scaled to the same distance and galactic reddening as SN 1988H.

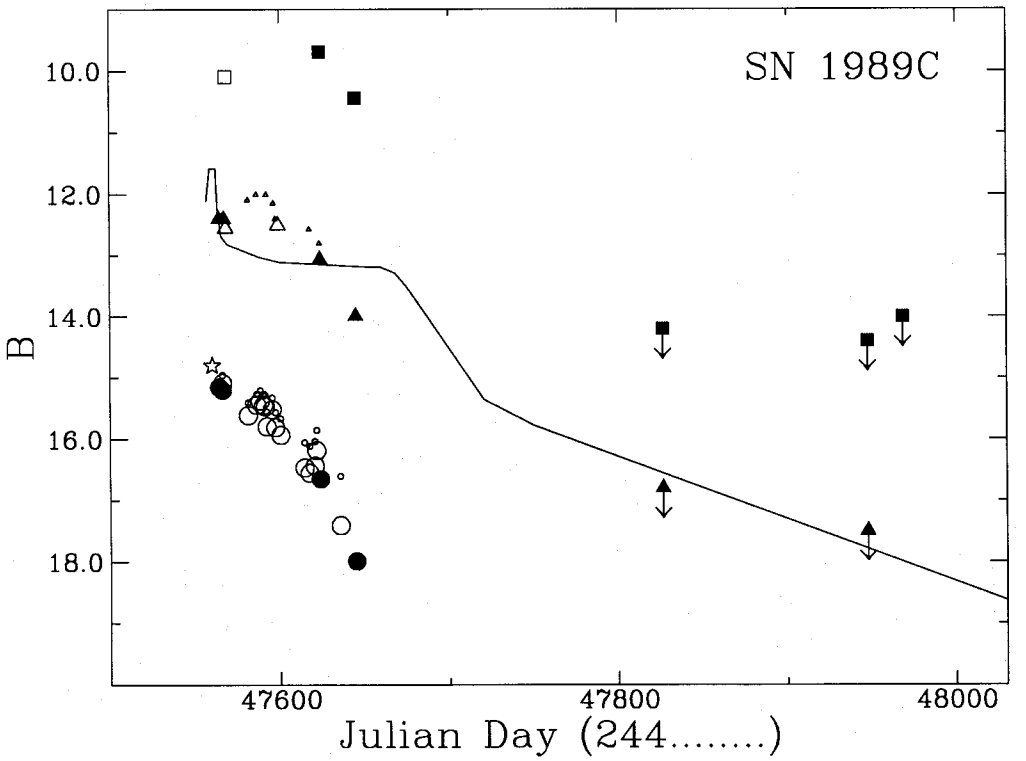

Figure 5. Light curves of SN 1989C in MGC+01-25-025. The vertical scale refers to *B* magnitudes (circles), while *V* data (triangles) have been upward-shifted by 3 mag and *R* data (squares) have been shifted by 6 mag. Filled symbols are data from Table 2, whereas open symbols are data from the literature. Small open circles and triangles are data from Kimeridze & Tsvetkov (1991), while large open symbols are the values corrected as described in Section 4.3. For comparison, the schematic *V* light curve of SN 1988A is also shown, scaled to the same distance and galactic reddening as SN 1989C.

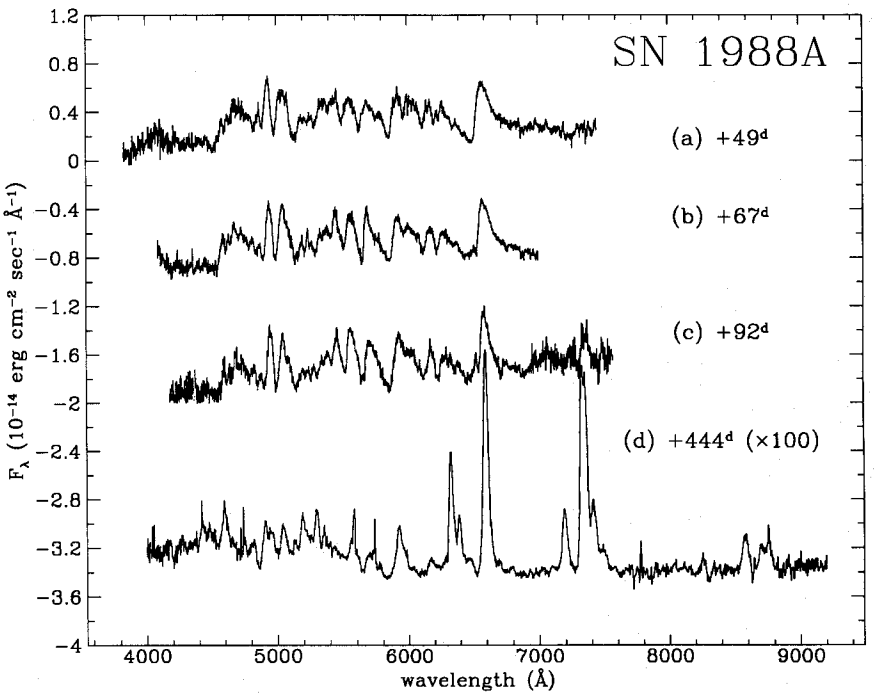

Figure 6. The spectral evolution of SN 1988A. The spectrograms (b) and (c) are the average of two observations taken on separate nights (Table 3). The flux scale is relative to spectrum (a), while the others have been shifted by −1, −2 and −3.5 units respectively. Spectrum (d) has been multiplied by 100.

Our spectra, from epochs 49 d to 444 d, are shown in Fig. 6. The general resemblance to the corresponding spectra of other type II SNe, in particular SN 1987A, is close, suggesting that SN 1988A is a rather normal SNII with respect to spectral appearance and temporal evolution. In the three earliest spectra, we believe that the strongest absorption features in the spectral range 4600–7000 Å are due to Hα, Hβ, Na I D, Mg I multiplet 2, Sc II multiplets 28, 29 and 31, and Fe II multiplets 42, 46, 49 and 74.

The most significant difference from SN 1987A is in the strength of the Ba II absorption lines in the first 100 d. It has been noted by Williams (1987) that the lines of these ions in SN 1987A are particularly strong, requiring enhancements for s-process elements (a factor of 5 for barium in Mazzali et al. 1992). In the available spectra of SN 1988A, Ba II 6142 Å at all epochs is weaker than for 1987A (but still present), while Sc II 6245 Å is possibly stronger. The Ba II 6497-Å line must also be present, and would complicate the structure of the P Cygni absorption in Hα. Chugai (1988) has questioned whether the barium line strength in SN 1987A is due to an abundance effect or whether the temperature is lower, creating an ionization balance with more Ba II at the expense of Ba III, in contrast to other type II supernovae such as SN 1988A. We note that Ba II has a significantly lower ionization potential than Fe II and that the $B-V$ colours of SN 1988A and most other type II supernovae are significantly bluer than those of SN 1987A in the interval 30–100 d after outburst.

Also different from SN 1987A is the presence of two weak lines at 6320 and 6390 Å, which make the blue profile of the Hα absorption less sharp. The relative ratios of these lines in SN 1988A are similar to those observed in SN 1986I (Pennypacker et al. 1989) and 1990H (preliminary reduction of the Asiago data).

The positions of the minima in the absorption lines with P Cygni profiles are commonly used for determining the envelope velocity, although in general for strong lines this would be expected to give a velocity greater than the photospheric velocity. In Table 4 are reported the velocities for the most prominent and hopefully relatively unblended lines, assuming for SN 1988A the same identification as for 1987A (Williams 1987). Although there is no overlap in epoch, our measurements are consistent with the analogous measurements by Schmidt et al. (1992) (note that their reference epoch is 11 d earlier than ours). The trend of the Na I D line is anomalous, probably because of contamination by other lines at later epochs. The Ba II lines also behave differently from others: the velocity from the 6142-Å line is the smallest and shows a negligible temporal evolution, while the velocity computed from the Ba II 4554-Å line, although less uncertain, varies more. This suggests that the Ba II 6142-Å line could be severely contaminated by absorption due to the Fe II 6149-Å line and by redshifted scattered photons from the Na I D lines (a possibility in SN 1987A also).

5.2 SN 1988H

Our spectra of SN 1988H were obtained on the same observing runs as those of 1988A and therefore correspond to earlier epochs (Table 3). Although poorly sampled, its spectral evolution (Fig. 7) is similar to that of SN 1988A, with the Ba II line weaker than in 1987A.

The expansion velocity (Table 4) is probably somewhat

Table 4. Expansion velocities for the absorption minima (km s^{-1}).

	Fe II		Sc II		Na I	Ba II		Hα
day	λ5018	λ5169	λ5526	λ5658	λ5893	λ4554	λ6142	λ6563
				SN 1988A				
49	3590	3370	3310	3190	3720	4220	2880	5020
67	3110	3080	2660	2560	3560	3560:	2690	
92	2630	2840	2170	2030	3770	2590:	2640	
				SN 1988H				
42	3890	3770		3650	5140			7220
68	3110	3310	3090		4630		2050	6170
				SN 1989C				
55	2990	2950	3770:	2960				4160
64	2690	2930	3260	3010		5010:		3840

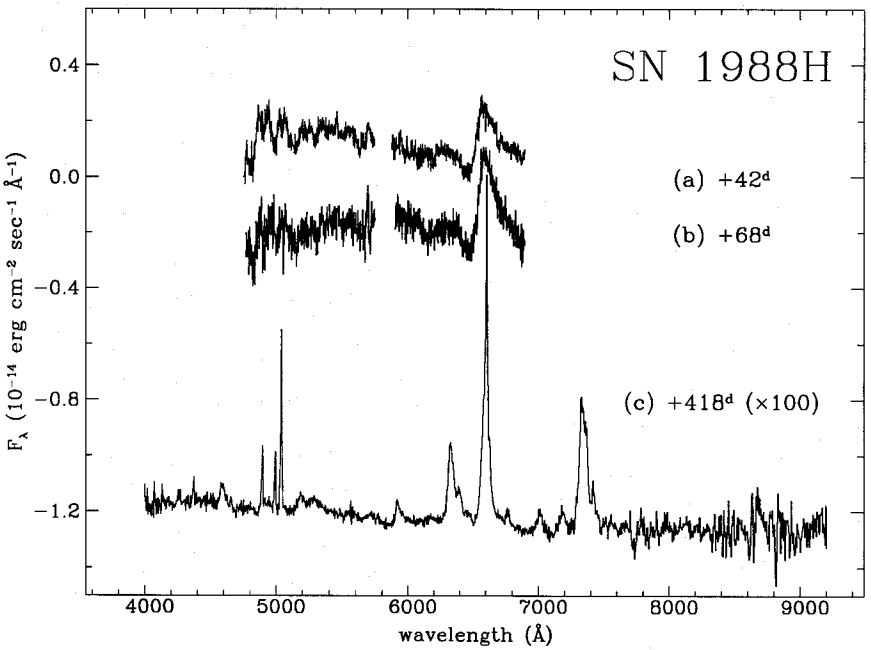

Figure 7. The spectral evolution of SN 1988H. The flux scale is relative to spectrum (a), while spectra (b) and (c) have been shifted by −0.3 and −1.3 units respectively. Spectrum (c) has been multiplied by 100.

higher than that of SN 1988A, with the highest value coming from Hα and the lowest from the line attributed to Ba II. At early stages the blueshift of the peak of Hα is very similar to that of SN 1988A, while the wings of the emission are somewhat broader. No sign of a blue emission feature is visible on the blue wing of the emission, but the signal-to-noise ratio is poor.

5.3 SN 1989C

On the basis of its early spectrum, SN 1989C has been included by Schlegel (1990) among the SNIIn. Several SNe have been proposed for this subclass, but to date only SNe 1987F, 1988I and 1988Z (Filippenko 1989; Turatto et al. 1993) have shown characteristics distinctly different from other SNII. Common properties are a particularly flat light curve, an Hα profile with a broad component on which is superposed a narrow peak, and no sign of P Cygni absorption (in 1988Z an intermediate-width emission component is also present). In Section 4.3 we concluded that the photometry of SN 1989C probably resembles that of a plateau SNII (or even a linear one) rather than the slowly evolving SN 1988Z.

The spectral evolution of SN 1989C in the first two months past maximum is shown in Fig. 8. The signal-to-noise ratio is better for later spectra, as larger telescopes were

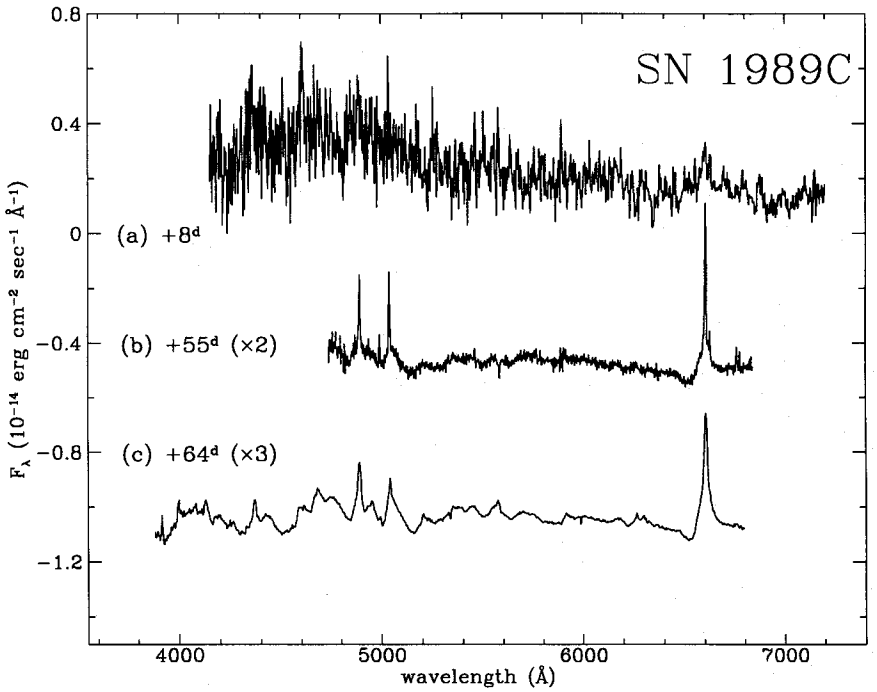

Figure 8. The spectral evolution of SN 1989C. The flux scale is relative to spectrum (b), while spectra (a) and (c) have been shifted by +0.7 and −0.6 units respectively.

used. The first noisy spectrum (epoch 8 d) shows only a broad Hα emission line on a blue continuum similar to the spectrum published by Schlegel (1990). Narrow emission lines are present.

About 50 d later the spectrum still shows a bluish continuum on which are superposed several unresolved (FWHM < 6 Å) lines. The most intense, the narrow Hα line, is on top of the broad Hα emission which now has a P Cygni profile. Other Balmer emission lines, as well as those of [N II], [S II] and [O III], are present, all at the recession velocity of the host galaxy. For these narrow lines, the Balmer decrement (Hα/Hβ∼ 2.8) and the other line ratios are typical of H II regions. This, together with the fact that the line intensities stay constant, suggests that they arise from a surrounding H II region rather than being associated with the SN.

The measurements of the envelope expansion velocities of SN 1989C are also reported in Table 4. Whereas for most of the lines the results are similar to those for the other two SNe at the same epoch, for Hα the velocities are significantly smaller. This was probably the reason for its inclusion by Schlegel (1990) in the class of SNIIn. If we accept that the unresolved component is due to contamination from a nearby H II region, it is also clear (Table 5) that the luminosity in the Hα line is, 2 months after maximum, factors of 4 and 10 fainter than in the SNe 1988A and 1988H respectively, while the *V* luminosities are similar.

5.4 The Hα line of SN 1988A

The rest-frame peak position and the integrated flux of the Hα emission for the three SNe are reported in Table 5. Also, to give an indication of the maximum expansion velocity within the H envelope, we have measured the width of the red wing of the emission (HWZI).

Note that, as found in several SNII (e.g. 1987A), in the early epochs the peak of the Hα emission is significantly blueshifted compared with the rest wavelength, in agreement with the theoretical prediction for this strong line (Jeffery & Branch 1990). Later the peak moves redward, although at a rate that varies from one SNII to another, and at late epochs reaches the rest wavelength.

In SN 1988A at 90 d past maximum the Hα emission was still in excess of 10 Å bluer than the rest position, while in SN 1987A it was already at the rest position 20 d after outburst (Hanuschik et al. 1988). However, at our latest epoch (444 d) the Hα emission peaked at its rest wavelength.

The expansion velocities deduced from the Hα absorption (Table 4) are not reported for epochs 67 and 92 d. In the spectra at epoch 67 d the profile of the absorption is complicated by an emerging emission feature at 6480 Å (Fig. 9), which is even clearer in the subsequent spectrum. Another weaker bump is present at about 6430 Å. We stress that at both epochs the spectra are the average of two independent observations, excluding the possibility of observational faults. Confirmation comes also from a spectrum of SN 1988A at a comparable epoch published by Filippenko (1991). No line is visible in that position, either in our spectrum at 444 d or in the spectra by Pearce et al. (1990) (∼ 142 d) and Sadler & Stathakis (1991) (∼ 190 d).

In Table 5 we report the main data for Hα and also for a feature that appears at the same wavelength in the spectra taken 20 d from the outburst of SN 1987A (Hanuschik et al. 1988; Phillips & Heathcote 1989). In analogy to SN 1987A, the peak drifts redward in a way similar to that of the photosphere (Table 4), and the velocity of the inner absorption (Phillips &

Table 5. Evolution of Hα profiles.

Day	Hα HWZI (Å)	Hα peak	Hα Total flux*	Blue Feature FWHM (Å)	Blue Feature peak	Blue Feature Flux ($F/F_{H\alpha}$)
			SN 1988A			
49	172	6540	22			
67	115	6542	30	23	6480	0.13
92	104	6553	30	17	6493	0.17
444	60	6563	0.8			
			SN 1988H			
42	250	6530	13			
68	220	6540	28			
418	60	6562:	0.4:	#		
			SN 1989C			
8	160:	6555:	15:	#		
55	80	6560	2.3	#		
64	85	6560	2.8	#		

* in units of 10^{-14}erg s^{-1} cm^{-2}; # only the broad component.

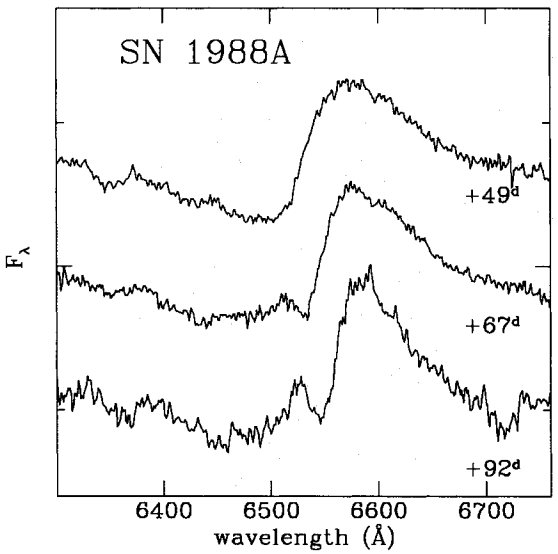

Figure 9. The evolution of the 6480-Å feature in SN 1988A.

Heathcote 1989) closely matches that of the photosphere as determined from the metal lines. The identification of these features is not certain. However, the emission feature on the blue wing of the Hα emission of SN 1987A (the Bochum event) lasted about 2 months and developed almost simultaneously with other features on the Hα red wing and in the IR hydrogen lines (Larson et al. 1987; Phillips & Heathcote 1989). These features have been variously interpreted as arising from density variations and/or ionization conditions in regions close to the photosphere (Hanuschik et al. 1988), or from selective line blanketing on the level population of hydrogen (Höflich 1988). However, since similar features appeared to be present in lines of other ions (e.g. the Na I D line), and because of the coincidence of the appearance of these features with the beginning of the tracking of the bolometric light curve by the Hα emission flux, the most promising interpretation is that they are associated with the penetration of radioactive material into the hydrogen envelope (Lucy 1988) and are seen as the photosphere recedes.

Following the suggestion by Hanuschik & Thimm (1990) that some of the emission features associated with the Bochum event may be due to lack of absorption, Chugai (1991) has developed a model for the appearance of the blueshifted feature in SN 1987A which can be plausibly applied to the case of SN 1988A. The model comprises two concentric layers of excited hydrogen, separated by a layer of unexcited hydrogen for which the optical depth is small. This structure can occur as a result of deep recombination of hydrogen at this epoch, and the presence of ^{56}Ni (and ^{56}Co) distributed throughout the envelope in clumps with a small volume filling factor. The inner layer is excited principally by photospheric emission, and the outer layer by non-thermal emission from radioactive decay. Absence of absorption in the intermediate zone arises because the photosphere is not effectively screened, due to the clumpiness of the radioactive material and the lower penetrating power of the exciting radiation at the high densities prevailing in this region. In this model the velocity of the inner P Cygni absorption should approximate the velocity of the photosphere (the precise relationship of course depends upon details of the model, such as the size of the envelope and the amount of emission and scattering). In fact, in SN 1988A this is what is observed when we compare these velocities with those from the absorption lines of the metals. The consequent reduction of this velocity as the photosphere recedes is expected and observed. Unfortunately, the lack of spectroscopic data at other epochs and the limited signal-to-noise ratio in other parts of our spectra prevent further testing of this model for SN 1988A. It seems plausible that the blueshifted structure near Hα reported for SN 1985L by Filippenko & Sargent (1986) has a similar physical cause.

These emission features in SN 1988A had disappeared by day 142 when Hα showed again a clear P Cygni profile (Pearce et al. 1990).

6 LATE-TIME SPECTRA OF SNe 1988A AND 1988H

Two high signal-to-noise ratio spectra of SNe 1988A and 1988H were obtained more than one year past maximum, well into the nebular phase (Fig. 10). At this epoch the envelope has become transparent and the inner layers of the stars are visible. The expansion velocities of these layers are relatively low, and the lines narrower, which makes the line identification easier.

Line identification was based on the coincidence of the peak of the emission (within ±10 Å) with lines selected on the basis of astrophysical considerations and given in Tables 6 and 7.

The general appearance of the spectra of the two SNe closely resembles that of the spectra of SN 1987A at the same epoch. The most intense lines are Hα, [O I], Ca II] and Ca II but they have smaller widths, i.e. they arise from slower emitting layers. For example, the [O I] and Hα lines, which are 55 and

70 Å wide in SN 1987A, have widths of 35 and 43 Å in SN 1988A and 40 and 54 Å in SN 1988H.

In both SNe the Balmer lines show a hint of P Cygni absorption, which might be present also in the Na I D line. The [O I] 6300–6363 Å lines are optically thin (intensity ratio 3:1). As expected from the progressive decrease in density, the intensity ratio of the Ca II] lines and the Ca II infrared triplet, which has values of ~ 1 and ~ 2 at about 200 d and 350 d past maximum (Sadler & Stathakis 1991), is now about 3.

Forbidden lines of Fe II are seen both in the blue and in the red. Allowed transitions of Fe II may also be present. A line at 6144 Å, which has been attributed to Na I, is present as a result of a fluorescence mechanism (Lucy et al. 1991b).

As in SN 1987A, in SNe 1988A and 1988H the Mg I] 4571-Å line is strong. In the spectrum of SN 1988A the Ca II 8662-Å line is blended with another emission line, which was identified in SN 1987A with [C I] 8727 Å. In our spectrum the coincidence of the observed line with the [C I] line is poor and a check on the [C I] 9824–9850 Å lines cannot be made because our spectra do not extend far enough.

In the spectrum of SN 1988H, in the same spectral region, a feature at 8621 Å is prominent. A similar feature in the spectra of SN 1987A after 700 d has been identified as [Fe II] 8617 Å (Spyromilio et al. 1991). The fact that in SN 1988H the same feature appeared 300 d earlier argues in favour of a faster evolution for this SN.

The strong [O I] lines and the implied high mass of oxygen suggest that the progenitors of both objects had masses greater than 12 $M_{\odot}$.

6.1 Dust formation in SN 1988H

The late-time spectrum of 1988H shows several unresolved lines, probably due to contamination by the adjacent H II region. In Section 3 we discussed the position of this SN and used a recession velocity at the location of the SN computed from these narrow emission lines. Table 7 shows that the wavelengths of the peaks of the SN broad emission lines relative to the rest-frame wavelengths reveal a blueshift that varies according to the line considered.

One possible explanation is that the narrow-line emitting region is not close to the SN. However, this seems unlikely, since the SN appears in the outer region of the host galaxy superimposed on a faint nebulosity which probably emits the narrow lines seen in the spectra. Also, the redshift deduced from the narrow lines is very close to that of the host galaxy (Table 1). In addition, the displacement of the SN lines seems too high to be due to peculiar motion.

Another more likely possibility is that the line profiles are distorted by dust extinction within the ejecta. The formation of dust in SNe several hundreds of days after the explosion has been unambiguously detected in SN 1987A (Danziger et al. 1991), in which the emission peaks of Mg I], [C I] and [O I] showed a clear blueward shift at 530 d past outburst, while the effect was considerably smaller for the hydrogen lines. This was an indication that the dust was formed mainly in the inner metal-rich envelope.

In SN 1988H, because of the sparseness of our data, we cannot follow the whole temporal evolution of the line profile as in SN 1987A. Nevertheless, we note that a significant blueshift is present for Mg I] 4171 Å (863 km s^{-1}), Na I D (588

Table 6. Spectral lines in SN 1988A (epoch 444 d).

λ_0 (Å)	ions	λ_{lab} (Å)	flux*
4407	[Fe II]	4402-4407	52
4459	[Fe II]	4452-4475	13
4574	Mg I]	4571	116
4885	Hβ	4861	104
4926	Fe II	4924	60
5022	Fe II	5018	91
5109	[Fe II]	5108	19
5164	[Fe II]	5158-5164	80
5190	Fe II	5198	
5230	Fe II	5235	4
5271	Fe II, [Fe II]	5259,5273	80
5326	Fe II	5317-5326	30
5551	[Fe II]	5551	150
5662	[Fe II]	5650	34
5745	[Fe II]	5747	16
5897	Na I D	5890-5896	268
6144	Na I:	6154-6161	36
6296	[O I]	6300	317
6358	[O I]	6363	106
6438	[Fe II], Fe II	6440,6442	35
6564	Hα	6563	840
6656	[Fe II]	6640-6658	22
7156	[Fe II]	7155	226
7301	Ca II]	7291-7324	1043
7373	[Fe II]	7373	167
7444	[Fe II]	7452	50
7531	[Fe II]:	7544	14
8538	Ca II	8542	140
8660	Ca II	8662	105
8713	[C I]:	8727	128

* in units of 10^{-17}erg s^{-1} cm^{-2}.

Table 7. Spectral lines in SN 1988H (epoch 418 d).

λ_0 (Å)	ions	λ_{lab} (Å)	flux*
4559	Mg I]	4571	28
4861	Hβ narrow	4861	23
4957-06	[O III] narrow	4959-5007	93
5156	[Fe II]	5158-5164	23
5249	Fe II, [Fe II]	5269,5273	27
5881	Na I D	5891-5896	30
6131	Na I:	6154-6161	6
6285-47	[O I]	6300-63	165
6422	[Fe II], Fe II	6440,6442	6
6555	Hα	6563	390
6718-31	[S II] narrow	6717-6731	10
6967	[Fe II]	6966-7011	53
7142	[Fe II]	7155	48
7296	Ca II]	7291-7324	321
7369	[Fe II]	7373	17
8621	[Fe II]	8617	49:

* in units of 10^{-17}erg s^{-1} cm^{-2}.

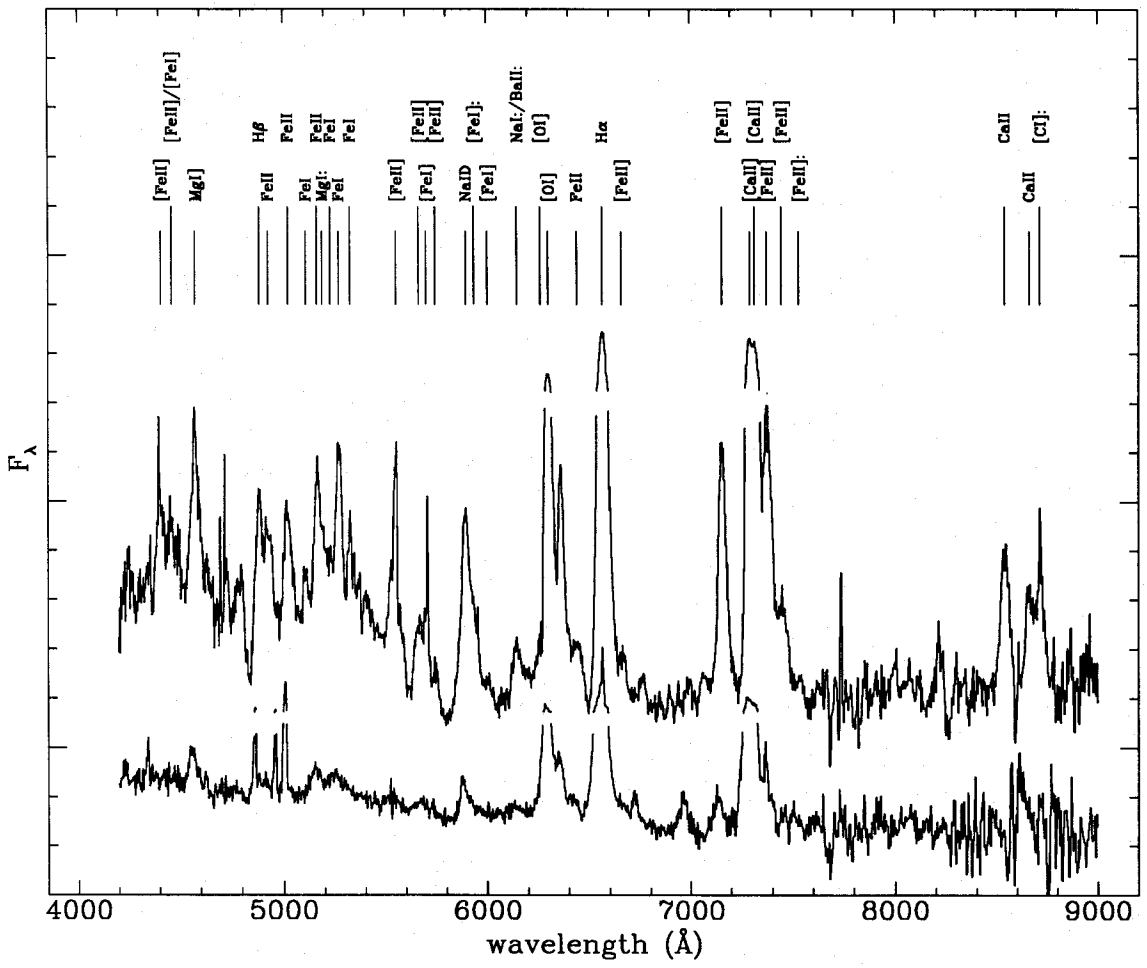

Figure 10. Comparison of the late-time spectra of SN 1988A (upper) and SN 1988H (lower) at about 400–450 d past maximum. The wavelength scale is in the SN rest frame. The identifications of the main features listed in Tables 6 and 7 are marked.

km s^{-1}), [O I] 6300 Å (581 km s^{-1}), [Fe II] 7155 Å (545 km s^{-1}) and Hα (153 km s^{-1}). In Fig. 11 we show an enlargement of the region of Hα, the strongest line. On it are superimposed the Gaussian fits of the broad component (based on the blue broad wing of the line) and the unresolved peak. The resulting fit shows a deficiency of radiation in the red wing compared with the Gaussian profile.

Assuming that the blue wing is unaffected by this extinction, we measure an absorption for the Hα flux of about 20–30 per cent. The amount of extinction by dust implied by the wavelength shift of the peak emission is approximately the same as recorded for SN 1987A. However, the dust in SN 1988H produces an optical depth in the visual at 5550 Å of $\tau_v \approx 1.2$ approximately 300 d earlier than in SN 1987A, if we simply adopt the model for the dust distribution proposed by Lucy et al. (1991a) for SN 1987A. We note that the dust in SN 1988H also has similar optical properties, as evidenced by the wavelength dependence of the velocity shifts. Furthermore, the significantly smaller shift for Hα demonstrates that in SN 1988H the dust was confined to the metal-rich interior and did not form in the outer hydrogen-rich layers. Although we lack IR data to support this conclusion, it is probably reasonable to expect that the dust is composed of small silicate grains.

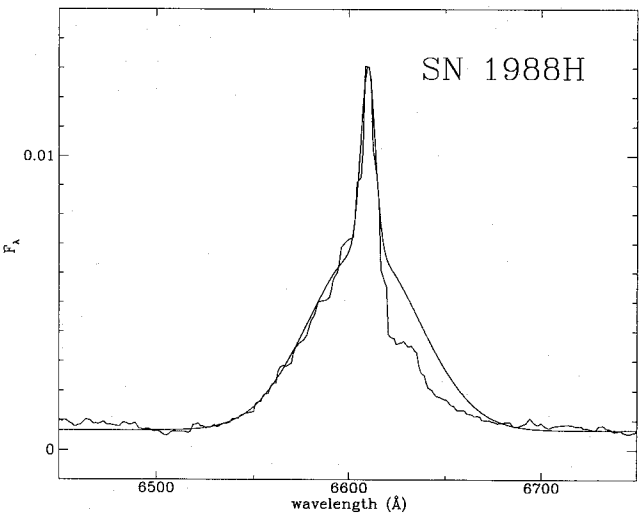

Figure 11. The profile of Hα in SN 1988H at epoch 398 d. On the observed spectrum is superimposed the fit with two components, the narrower due to contamination by the H II region, and the broader based only on the blue wing of the emission. The deficiency shown by the red wing is attributed to extinction by dust within the ejecta.

7 CONCLUSIONS

In this paper we have presented new late-time photometry and spectroscopy of SN 1988A. The broad-band photometric observations show that, contrary to previous claims, no additional sources of energy are necessary to power the light curve at least up to 800 d past maximum. Inconsistencies among the data from different authors are ascribed to inadequate subtraction of the host galaxy background. Late-time spectroscopy of SN 1988A has revealed emission lines narrower than in 1987A at similar epochs. Apart from the lines of H, [O I], Ca II, Na I and Mg I] there are many others, some fraction of which must be due to [Fe II] and possibly Fe II.

A spectrum of SN 1988H at a similar epoch resembles that of SN 1988A. Nevertheless, the positions of the broad lines are blueshifted with respect to the rest position by amounts which depend upon the wavelength of the line. Moreover, the line profiles are asymmetric with a deficiency of radiation in the red wings, indicating the presence of dust in the SN ejecta prior to day 418. The amount of obscuration is similar in magnitude and nature to that in SN 1987A, although it occurs at least 100 d earlier and reaches an optical depth of ~ 1.2 in the visual at least 300 d earlier. One might conjecture that the earlier formation of dust in SN 1988H results from the significantly higher expansion velocities [see Hanuschik & Schmidt-Kaler (1989) for expansion velocities of SN 1987A corresponding to the epochs presented in Table 4 above]. Thus SN 1988H would achieve the conditions necessary for dust formation earlier. Clearly, other factors such as chemical composition of the envelope (for which we have little detailed information) might be expected to play a role. Inspection of Table 4 reveals that the early expansion of SN 1988A was slower than that of SN 1988H. Perhaps this could be the primary reason why dust had not formed in SN 1988A as late as day 444. Unfortunately, the late-time light curve is scarcely defined and a deviation from the exponential tail, as seen in SN 1987A, could not be detected.

The paper also discusses new observations of SNe 1988A and 1988H obtained shortly (within 3 months) after the outbursts. The spectra of SN 1988A, whose photometry was studied in a previous paper (Benetti et al. 1991), show the appearance between 60 and 100 d of emission structures in the P Cygni absorption trough of Hα, which could be interpreted as signatures of the penetration of radioactive material above the photosphere, in analogy to similar structure observed in SN 1987A. Sparse photometry and spectra of SN 1988H show that its behaviour is typical of a plateau SNII.

The case of SN 1989C is interesting because it was proposed to belong to the so-called SNIIn class. New CCD photometry has shown that the previously published data following maximum light were progressively contaminated by the light of the galaxy nucleus near which the SN appears. The revised light curve is steeper than previously thought but still shows a definite plateau. Three spectra sample the first 2 months of evolution. The early spectrum appears relatively blue but the general appearance is normal. The fluxes of the narrow lines already noted in other spectra of this object did not change, and the relative intensities seem to indicate that they arise from an underlying H II emission region rather than from the SN. The low expansion velocities derived from the Hα absorption minima are abnormal. In SN 1989C, unlike other SNII, these velocities are similar to those of the photosphere derived from Fe II lines and thus indicate a lower optical depth of hydrogen.

ACKNOWLEDGMENTS

We are indebted to S. Ortolani, who provided the observations of SN 1988A in 1990 March. IJD is especially grateful to N. Chugai for many illuminating discussions.

REFERENCES

Benetti S., Cappellaro E., Turatto M., 1991, A&A, 247, 410
Cappellaro E., Turatto M., Benetti S., Tsvetkov D.Yu., Bartunov O.S., Makarova I.N., 1993, A&A, 273, 383
Cappellaro E., Della Valle M., Iijima T., Turatto M., 1990, A&A, 228, 61
Chugai N.N., 1988, Sov. Phys. Usp., 31, 775
Chugai N.N., 1991, SvA, 17, L400
Danziger I.J., Fosbury R.A.E., Alloin D., Cristiani S., Dachs J., Gouiffes C., Jarvis B., Sahu K.C., 1987, A&A, 177, L13
Danziger I.J., Bouchet P., Gouiffes C., Lucy L.B., 1991, in Danziger I.J., Kjär K., eds, Supernova 1987A and other Supernovae. ESO Workshop and Conf. Proc. No. 37, ESO, Garching, p.217
Filippenko A.V., Sargent W.L.W., 1986, AJ, 91, 691
Filippenko A.V., 1989, AJ, 97, 726
Filippenko A.V., 1991, in Danziger I.J., Kjär K., eds, Supernova 1987A and other Supernovae. ESO Workshop and Conf. Proc. No. 37, ESO, Garching, p.343
Hanuschik R.W., Thimm G., Dachs J., 1988, MNRAS, 234, 41P
Hanuschik R.W., Schmidt-Kaler Th., 1989, MNRAS, 241, 347
Hanuschik R.W., Thimm G., 1990, A&A, 231, 77
Höflich P., 1988, Proc. Astron. Soc. Aust., 7, 434
Jeffery D., Branch D., 1990, in Wheeler J.C., Piran T., Weinberg S., eds, Supernovae. World Scientific Publishing Co., Singapore, p.149
Kimeridze G.N., Tsvetkov D.Yu., 1991, AZh, 68, 341
Landolt A.U., 1983, AJ, 88, 439
Larson H.P., Drapatz S., Mumma M.J., Weaver H.A., 1987, in Danziger I.J., ed., SN 1987A. ESO Workshop and Conf. Proc. No. 26, ESO, Garching, p.147
Lucy L.B., 1988, in Kafatos M., Michalitsianos A.G., eds, Supernova 1987A in the Large Magellanic Cloud. Cambridge Univ. Press, Cambridge, p.323
Lucy L. B., Danziger I. J., Gouiffes C., Bouchet P., 1991a, in Woosley S. E., ed., Supernovae. Springer-Verlag, New York, p.82
Lucy L.B., Danziger I.J., Gouiffes C., 1991b, A&A, 243, 223
Mazzali P.A., Lucy L.B., Butler K., 1992, A&A, 258, 399
Miller D.L., Branch D., 1990, AJ, 100, 530
Patat F., Barbon R., Cappellaro E., Turatto M., 1993, A&AS, 98, 443
Pearce G., Patchett B.E., Allington-Smith J.R., 1990 Ap&SS, 166, 41
Pennypacker C.R. et al., 1989, AJ, 97, 186
Perlmutter S., Pennypacker C., Djorgovski S., Meylan G., 1988, IAU Circ. 4560
Phillips M.M., Heathcote S.R., 1989, PASP, 101, 137
Ruiz-Lapuente P., Kidger M., Lopez R., Canal R., 1990, AJ, 100, 782
Ruiz-Lapuente P., Kidger M., Gomez G., Canal R., Lopez R., 1991, ApJ, 378, L41
Sadler E.M., Stathakis R.A., 1991, in Danziger I.J., Kjär K., eds, Supernova 1987A and other Supernovae. ESO Workshop and Conf. Proc. No. 37, ESO, Garching, p.331
Schlegel E.M., 1990, MNRAS, 244, 269
Schmidt B.P., Kirshner R.P., Eastman R.G., 1992, ApJ, 395, 366
Spyromilio J., Stathakis R. A., Cannon R. D., Waterman L., Couch W. J., Dopita M. A., 1991, MNRAS, 248, 465
Stathakis R.A., Sadler E.M., 1991, MNRAS, 250, 786

Tully R.B., 1988, Nearby Galaxies Catalog. Cambridge Univ. Press, Cambridge
Turatto M., Cappellaro E., Barbon R., Della Valle M., Ortolani S., Rosino L., 1990, AJ, 100, 771
Turatto M., Cappellaro E., Danziger I.J., Benetti S., Gouiffes C., Della Valle M., 1993, MNRAS, 262, 128
Wild P., 1989, IAU Circ. 4730
Williams R.E., 1987, ApJ, 320, L117

This paper has been produced using the Blackwell Scientific Publications LaTeX style file.